Thin-film crystalline silicon on glass

Joke M. Westra and Miro Zeman

Abstract—**The aim of this research project is to develop technology for thin-film crystalline silicon solar cells on glass, which combines the high efficiency of crystalline silicon based solar cells with the low temperature processing of amorphous silicon (a-Si) thin films. In this work we focus on the realization of device-quality thin-film c-Si on glass by crystallization of thin a-Si films. Expanding thermal plasma chemical vapor deposition (ETP CVD) has the potential for fabricating good quality thin a-Si films at deposition rates ten times higher than plasma enhanced CVD a-Si layers of similar quality. A-Si films of 2 µm were deposited by ETP CVD at a deposition rate of 0.8 nm/s. The a-Si films were crystallized by means of solid phase crystallization.**

In this work the relation between the a-Si film quality and the quality of c-Si film after crystallization was investigated. A series of a-Si depositions was carried out at temperatures of 200 ºC, 300 ºC and 400 ºC. The deposition temperature strongly influenced structural properties of the a-Si, such as the hydrogen content. The silicon films were characterized by Fourier transform infrared spectrometer and Raman spectroscopy to evaluate the hydrogen content and structural properties before and after crystallization. Further evaluation of the crystalline structure of the c-Si films was carried out by x-ray diffraction.

Index Terms—**Crystallization, Silicon, Solar Cell, Thin Film**

I. Introduction

In the last decade the production of solar cells has increased dramatically. Since 2005 this market's average annual growth has been 40%, making it one of the fastest growing industries [1]. Today's terrestrial PV market is dominated by crystalline silicon (c-Si) solar cells based on wafer technology, known as the "first generation" solar cells, which accounts for 90% of the world production of solar cells [2]. In order to maintain the rapid expansion of the solar cell sector, reduction of solar cell costs is required. The cost of c-Si modules is dominated by materials costs, mainly the cost of the c-Si wafers. A significant cost reduction can be achieved by reducing the consumption of highly pure c-Si. Wafer thicknesses used in the solar cells are around 220 µm. These wafers are sawn from ingots. In the sawing process additional c-Si material is lost as a waste that amounts to about 50% of the wafer thickness. One of the main functions of the wafers is mechanical support. In the upper 30 µm of the wafer most of the optical absorption occurs [2]. This provides the possibility for reducing the silicon thickness without compromising the high efficiencies. Several approaches have been considered to reduce the amount of crystalline silicon in cells; these include cutting thinner wafers and thin-film solar cell approach. The optimization of cutting to reduce the material consumption is limited by the cutting losses, which are not reduced as the wafer thickness decreases.

Thin-film solar cells are known as the "second generation" solar cells. A significant decrease in material consumption makes thin-film solar cells a promising option for cost reduction. Although several photovoltaic materials are suitable for thin-film solar cells, the most promising material from long-term perspective is silicon. Hydrogenated amorphous silicon (a-Si:H) and microcrystalline silicon (µc-Si) are already used in commercial solar cells. A typical structural feature of µc-Si is that it has small crystalline grains (>100 nm). Both materials are commonly fabricated using plasma enhanced CVD (PECVD) at temperatures below 300 ºC. Unfortunately the a-Si:H and µc-Si films cannot compete with the opto-electrical properties of c-Si and therefore solar cells with a-Si:H and µc-Si absorber layers yield poorer performance than solar cells based on c-Si.

If the wafers in solar cells are replaced by thin film materials, the mechanical load has to be carried by another material. Glass is most used as substrate, because of its transparency, stability, and low cost. Unfortunately the processing temperature of the glass is limited by its softening that occurs above 650 ºC. As this project deals with thin-film c-Si solar cells on glass, the processing temperature is limited by 650 ºC.

The first goal of the project is to develop device grade crystalline silicon thin films. Large-grained polycrystalline silicon is required for solar cells. The grains size must be larger than the film thickness and the intra-grain material quality should be comparable to wafer based polycrystalline silicon. The last requirement entails that the amorphous fraction between the grains should be minimized and the presence of voids is unwanted as these are detrimental to the solar cell performance. The preparation of such large-grained polycrystalline Si films is a serious challenge due to the glass substrate limitations [2].

Manuscript received October 1, 2008. This work was supported by the Dutch Ministry of Economic Affairs under the SenterNovem EOS-LT program (project number EOSLT06029) and is carried out in cooperation with Eindhoven University of Technology.

J. M. Westra is with the Laboratory of Electrical and Computer Engineering, DIMES Technology Centre, Delft University of Technology, Feldmannweg 17, 2628 CT Delft, The Netherlands. (phone: +31 (0)15-86288; e-mail: j.m.westra@tudelft.nl).

M. Zeman is with the Laboratory of Electrical and Computer Engineering, DIMES Technology Centre, Delft University of Technology, The Netherlands.

The second goal of the project is to apply the thin crystalline silicon layer as an absorber in a solar cell. It could be applied in both homo- and heterojunction cells. Due to the low temperature processing of the heterojunction cell, this type of cell is preferred. Another reason is the good solar cell performance using heterojunction approach on c-Si wafers [4].

The crystalline silicon thin film can be made by a two step process which consists of a deposition of a-Si film and its crystallization. CSG company has applied this approach and developed crystalline silicon on glass solar cells (CSG) based on thermal SPC of PECVD a-Si with conversion efficiencies of 10.4% [5]. This technology has been already implemented in industrial production [6]. Another method for crystallization is rapid thermal annealling (RTA). RTA is mostly used at high temperatures (800-1100 ºC) [6, 7]. Crystallization can be achieved through RTA also at low temperatures, unfortunately it requires prolonged time (200 to 60 hours at 600 ºC) [8]. SPC is used more often at temperatures around 600 ºC, which can induce complete crystallization in 5-7 hours [9] and can be used in combination with metal induced crystallization [10]. In this project the Expanding Thermal Plasma (ETP) CVD is used as a fast deposition of a-Si films that are suited for crystallization. The a-Si films can be grown at deposition rates up to 11 nm/s [11]. SPC has been used to crystallize a-Si films deposited by other techniques, such as e-beam deposition [12] and rf-PECVD deposition [5]. A-Si films deposited by these methods require long annealing time or have lower deposition rates when compared to ETP CVD. A-Si films deposited by ETP CVD can be transformed to high crystalline quality films by SPC at 650 °C within several hours [11]. Because the combination of ETP CVD with SPC has the possibility of a higher throughput than alternative methods, these two techniques will be combined in this project.

II. EXPERIMENTAL METHODS

A. Expanding thermal plasma (ETP) CVD

The deposition of amorphous silicon is carried out in the CASCADE deposition set-up (Fig. 1). The ETP CVD method was developed by Eindhoven University of Technology. The ETP CVD is a remote plasma technique, this means that the creation of the plasma, the transport, and the deposition occur separately in different parts of the set-up.

The dc thermal arc plasma source induces an arc discharge through a channel. The channel is built up of six copper plates with an orifice in the centre. The plates are electrically isolated from each other by boron-nitride discs and O-rings. The plasma is created using three cathodes in the top of the arc and a copper plate (anode) at the bottom of the arc (Fig. 2). Non-depositing gases are used to create the plasma, the discharge is controlled by the current. The gasses that are used are argon and hydrogen, the current is usually 40 A. The power dissipated in the arc is typically within 5 and 8 kW.

The cascaded arc has a high pressure, of approximately 45×10^3 Pa. The plasma emanates from the arc. It continues through a conical nozzle and expands into the deposition chamber. The pressure in the deposition chamber is approximately 20 Pa. The supersonic expansion occurs due to the large pressure difference between the arc and the chamber.

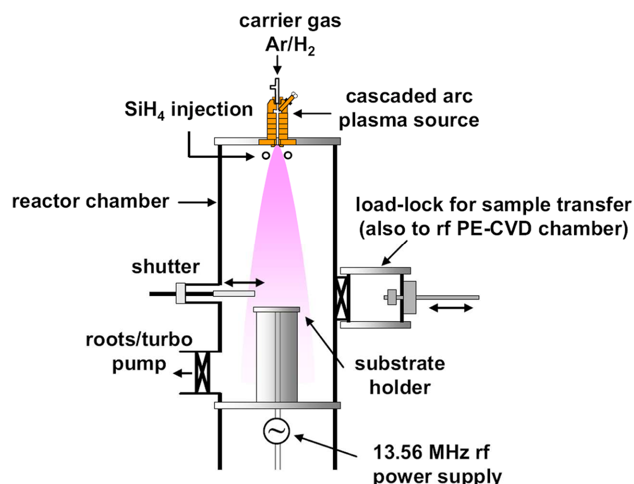

Fig. 1. Schematic of the ETP CVD, Cascade deposition equipment.

The plasma expands sub-sonically after a stationary shock, just a few centimeters from the arc outlet. The velocity of the reactive ionic and atomic species after the shock is typically 1000 m/s. Examples of the ionic and atomic species are Ar+ and H, and their velocity decreases to zero at the stagnation point [14][15].

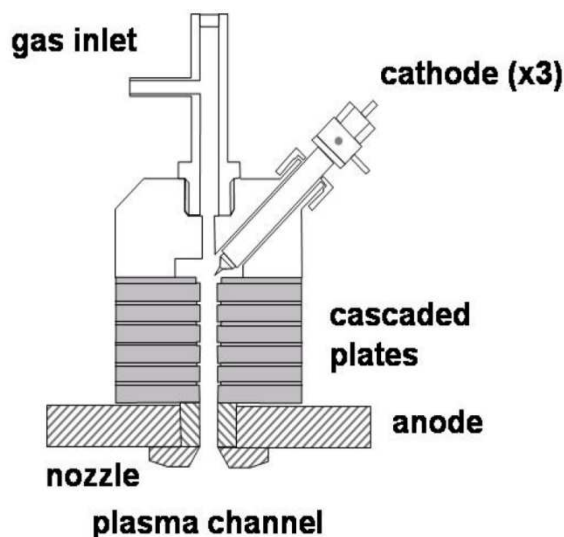

Fig. 2. Detail of the cascaded arc plasma source.

The current ETP CVD set-up in Delft, called CASCADE, was built in a joint project of Delft and Eindhoven Universities of Technology. The set-up consists of two reaction chambers (one for rf PECVD and one for ETP) that are connected via a load lock. The equipment has been used to produce device grade a-Si:H films at deposition rates up to 10 nm/s at substrate temperatures below 500 ºC [6]. These films were used for thin film a-Si:H based solar cells.

B. Spectroscopic Ellipsometry (SE)

The CASCADE is equipped with a spectroscopic ellipsometer. Spectroscopic ellipsometry (SE) is an optical technique based on the interaction of matter with monochromatic polarized light [16]. The technique uses the reflection of light from the layer surfaces to characterize the dielectric properties of these layers (Fig. 3). In SE the change in the dielectric function is related to the thickness and roughness of the deposited layer. The analysis of the signal is based on a comparison of the measured signal with an estimation of change in the dielectric function. This estimation is based on a model that takes into account the influences of different layers on the overall dielectric function. The results from the model are compared and fitted to the measured dielectric function. The model is used to evaluate the deposition rate and final thickness of the material.

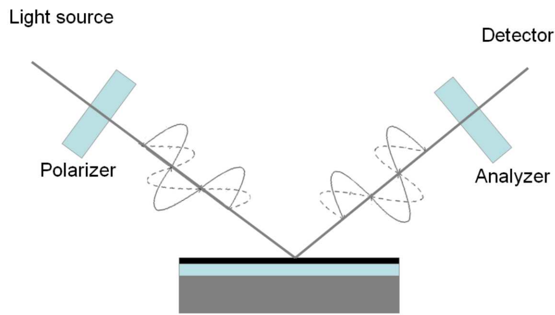

Fig. 3. The light of the SE source will interact with each layer in a material structure, this sketch shows which layers are included for the interpretation of the detected SE signal.

The layers for which the changes in dielectric signal are simulated are the substrate material, one layer of amorphous silicon and the surface roughness. The dielectric function of the substrate material is determined prior to deposition, by measurements at the deposition temperature. These measurements are used to model the behavior of the substrate layer in the multilayer model. The roughness and film thickness are modeled from experience. By means of an ex-situ reflection and transmission measurement the final thickness is evaluated and compare to the final thickness calculated by the SE model.

C. Fourier transform infrared (FTIR) spectrometry

FTIR is used mostly in chemical analysis. The signal that is measured is the direct Fourier transform of the IR spectrum; which is the intensity of IR radiation for a range of wave numbers (cm^{-1}). A computer calculates and plots the actual IR spectrum. The absorption peaks in the infrared transmission spectrum correspond to the vibrational mode of specific chemical bonds. The density of these bonds can be calculated from the area of the peak. The peaks related to hydrogen bonds are used to evaluate the amount of hydrogen present in the material. The vibrational mode at 640 cm^{-1} can be used to determine the total hydrogen density of the material, as every hydrogen atom bonded to the silicon network contributes to this peak. The vibrational mode at 2000 cm^{-1} mode corresponds to monohydride SiH bonding [17], whereas the 2100 cm^{-1} mode is usually is associated with dihydride SiH_2 bonding, clustered hydrogen and monohydride bonds on internal surfaces of voids [9].

The vibrational modes centered at ~ 1980-2010 and ~ 2070-2100 cm^{-1} are called the low stretching mode (LSM) and high stretching mode (HSM), respectively. The microstructure parameter, R*, is a figure of merit for the hydrogen microstructure of a material and is defined as:

$$R^* = \frac{I_{HSM}}{I_{LSM} + I_{HSM}} \quad (1)$$

where I_{LSM} and I_{HSM} are the integrated absorption strength of the low and high stretching modes, respectively. An R* value below 0.1 is generally found in device quality a-Si:H [18, 19].

D. Solid Phase Crystallization (SPC)

The SPC takes place in a horizontal tube furnace operating at temperatures around 650 ºC. Heating rate is possible up to 20 ºC/s. No cooling installation is present. The furnace is used at low pressure (10^{-2} Pa). The tube furnace is not yet equipped with any in-situ measuring equipment.

E. Raman spectroscopy

Crystalline silicon has a very specific Raman spectrum and for this reason, the Raman spectroscopy is employed for a fast evaluation of the crystallization of the silicon films after SPC.

The Raman effect occurs due to the interaction of light with a material. To induce this effect a monochromatic light source (laser) is used excite the electrons in the crystal, and a spectrogram of the scattered light shows the deviations in reference to the monochromatic light. These deviations are the result of the transition of electrons from their excited states to lower energy state of the crystal. So the increase intensity measured at specific wavelengths is characteristic for the states present in a crystal structure. In Raman spectroscopy a shift in frequency can be observed due to stress in the material or by chemical bonding. An increase in frequency can be found with compressive stress and a decrease with tensile stress. Crystalline silicon exhibits a typical Raman signal at a frequency of about 520 cm^{-1}.

Important to note is that the measured intensity is dependent on the calibration of the system. This means that the relative shifts can be observed with great accuracy, but the intensity is not reliable as an absolute measurement [20, 21].

F. X-ray diffraction (XRD)

The theory of X-ray diffraction is based on measurement of the lattice spacing of crystallites which satisfy the Bragg condition for a particular reflection. The most pronounce peaks of the XRD pattern of c-Si belong to the (111), (200) and (311) crystallographic planes. Amorphous materials do not give sharp peaks in the diffraction spectrum; therefore XRD can be used to evaluate the degree of crystallinity [22].

III. Experimental details

A. Deposition and crystallization of silicon films

In these experiments a series of amorphous silicon films with a thickness of 2 µm are deposited by ETP CVD, using the Cascade set-up, described earlier. The gasses used in the deposition are argon, hydrogen, silane, and helium. The first two gases are used primarily for the plasma, silane is used as a source of silicon and helium is used for a homogeneous heat distribution. The substrate temperature is varied throughout the experiment. The series consists of the depositions made at substrate temperatures of 200, 300 and 400 ºC. All other settings remain constant.

The crystallization process is the same for all samples. The procedure consists of a temperature ramp up of 10 ºC/min until 400 ºC is reached, then the heating is continued by 2 ºC/min up to 650 ºC. At 650 ºC the temperature is kept constant for 30 min, after which the samples are left to cool down slowly until they reach room temperature (25 ºC).

A. Characterization

The deposition of amorphous films was monitored in situ by the SE equipment. The hydrogen content of the amorphous films was determined by FTIR, the results of the FTIR were used to determine the microstructure parameter R*. The degree of crystallinity after SPC was examined by Raman spectroscopy and XRD.

IV. Results

The deposition rates, as observed with spectroscopic ellipsometry, were approximately constant for the whole duration of the deposition. The deposition rate was slightly lower for higher substrate temperatures.

The hydrogen content and the values for the microstructure parameter R* obtained from the FTIR are shown in table I. An example of a raw FTIR spectrum of an amorphous film is shown below (Fig. 4).

TABLE I
RESULTS FOR TEMPERATURES SERIES OF 2 MICROMETER THICKNESS

Deposition temperature (ºC)	Deposition rate (nm/s)	Hydrogen content (at %)	R*
400	0,71	5,33	0,22
300	0,78	7,37	0,20
200	0,79	12,10	0,53

After SPC the films were examined by Raman spectroscopy and XRD. The Raman spectrum of each sample showed a strong peak near 520 cm^{-1} (Fig. 5). The XRD results show the background signal of glass and high intensity peaks which are related to the crystallographic directions of silicon (Fig. 6).

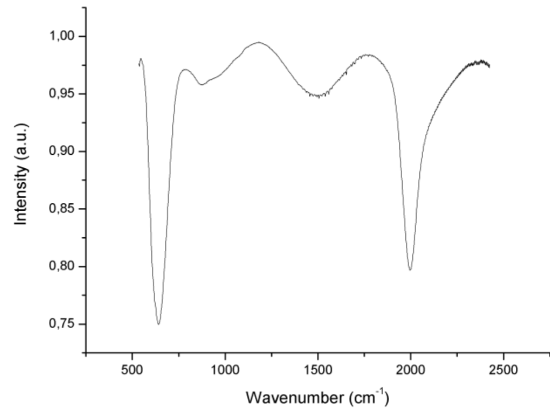

Fig. 4. A raw FTIR spectrum of an amorphous silicon film, which was deposited at 400 ºC substrate temperature, by ETP CVD.

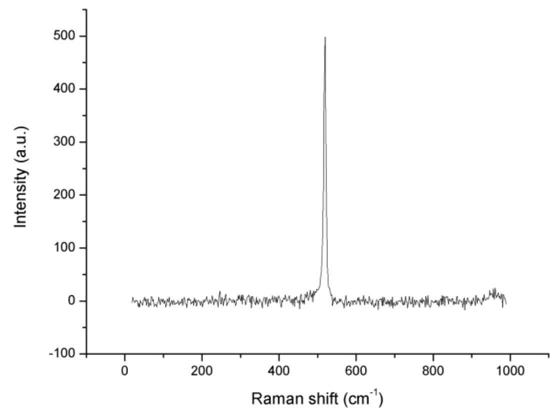

Fig. 5. Raman spectrum of a crystallized sample which was deposited by ETP CVD, at 400 ºC substrate temperature.

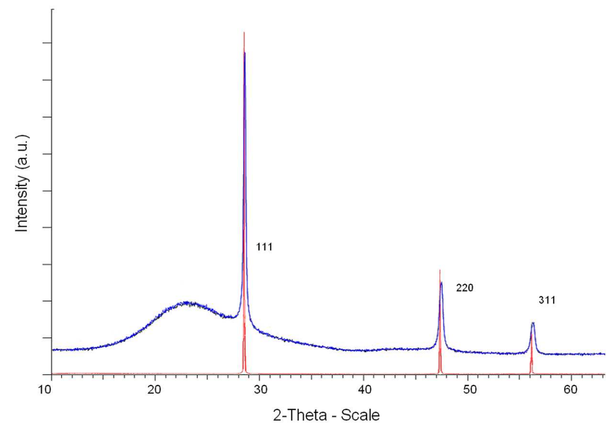

Fig. 6. The blue line is a XRD spectrum of a crystallized sample on a glass substrate, which was deposited at 400 ºC by ETP CVD. The red line is a stress free, mono-crystalline reference sample, without glass. The numbers next to the peaks indicate the crystallographic direction of the measured peak.

V. Discussion and conclusion

The change in the growth rate is related to the different substrate temperatures, it decreases with increasing substrate

temperature. The substrate temperature has an influence on both the hydrogen content and the microstructure parameter R*. The R* of a-Si:H films is larger than device quality a-Si:H films used as absorber layers in solar cells [19]. This increase in R* indicates unfavorable structural properties of a-Si:H layers which can affect the degradation behavior of solar cell with these absorber layers. However, these a-Si films with insufficient quality for a-Si thin film solar cells might still be good candidates for the production of device grade c-Si thin films.

The Raman and XRD spectra for all crystallized Si films show similar patterns. Results from both techniques demonstrate that crystallization has been accomplished. The relation between the amorphous and crystallized layers shows that a-Si films deposited at various temperatures by ETP are suitable for crystallization by SPC.

ACKNOWLEDGMENT

The authors would like to thank M. Tijssen and K. Zwetsloot for technical assistance during sample preparation. K. Sharma and A. Illibri are acknowledged for their help with the SPC set-up. N. van der Pers at the Department of Materials Science and Engineering of the Delft University of Technology is acknowledged for the X-ray analysis.

REFERENCES

[1] W. Hoffmann, "PV solar electricity industry: Market growth and perspective," *Solar Energy Materials & Solar Cells*, 2006, vol. 90, pp. 3285–3311.

[2] S. Gall, et al., "Large-grained polycrystalline silicon on glass for thin-film solar cells," *Thin solid films,* 2006, vol 511-512, pp. 7-14.

[3] P.A. Bassore, "Simplified processing and improved efficiency of crystalline silicon on glass modules," *19th European PVSEC*, Paris, June 2004, pp. 455-458.

[4] T. Sawada et al., "High-efficiency a-Si/c-Si heterojunction solar cell," in *Proc 1st WCPEC;* Hawaii, 2004, pp. 1219-1226.

[5] M.A. Green et al., "Crystalline silicon on glass (CSG) thin-film solar cell modules," *Solar Energy*, 2004, vol. 77 pp. 857-863.

[6] M.J. Keevers et al., "10% Efficient CSG minimodules," in *Proc. 22nd EPVSEC*, Milan (Italy), 2007, pp. 1032-1040.

[7] A.T. Fiory, "Methods in rapid thermal annealing," in *Proc.* 8th *Int. Conf. on Adv. Thermal Proc. of Semiconductors*, Gaithersburg, 2000, pp. 15-25.

[8] K. Pangal, "Hydrogen plasma enhanced crystallization of hydrogenated amorphous silicon films," *J. of Appl. Phys.* 1999, vol. 85(3), pp.1900 - 1906.

[9] R.B. Bergmann et al., "Solid-phase crystallized Si films on glass substrates for thin film solar cells." *Solar Energy Materials and Solar Cells*, 1997, vol. 46, pp. 147 - 155.

[10] W. Fuhs et al., "A novel route to a polycrystalline silicon thin-film solar cell," *Solar Energy*, 2004, vol. 77, pp. 961-968.

[11] M.C.M. van de Zanden, et al., "A novel approach for thin-film polycrystalline silicon on glass," in *Proc. MRS Symp. P: PV Mat. Manu. Issues*, 2008, to be published.

[12] D. Song et al. "Solid phase crystallized polycrystalline thin-films on glass from evaporated silicon for photovoltaic applications," *Thin Solid Films*, 2006, vol. 513, pp. 356–363

[13] R. Brendel, D. Scholten, "Modeling light trapping and electronic transport of waffle-shaped crystalline thin-film Si solar cells : Thin film solar cells," *Appl. Phys., A Mater Sci Process*., 1999, vol. 69(2), pp. 201-213

[14] A. Petit, "Expanding Thermal Plasma Deposition of Hydrogenated Amorphous Silicon for Solar Cells," Ph.D. dissertation, Dept. Elect. Eng., Delft Univ. of Tech., 2006, ch. 2.

[15] C. Smit et al., "Fast deposition of microcrystalline silicon with an expanding thermal plasma," *J Non-Cryst. Solids*, 2002, vol. 299-302(1), pp. 98-102.

[16] A.E. Irene, "Surfaces Interfaces and Thin films for Microelectronics," Wiley-Interscience, Portland OR, 2008, ch 9.

[17] J.C. Knights, G. Lucovsky and R.J. Nemanich, "Defects in plasma-deposited a-Si: H," *J. Non-Cryst. Solids*, 1979, vol. 32, pp. 393-403.

[18] G. Lucovsky, R.J. Nemanich and J.C. Knights, "Structural interpretation of the vibrational spectra of a-Si: H alloys." *Phys. Rev. B*, 1979, vol. 19 pp. 2064-2073.

[19] R.E.I. Schropp, M. Zeman, "Amorphous and Microcrystalline Silicon Solar Cells, Modeling, Materials, and Device Technology," Kluwer Academic Publishers, Dordrecht, 1998.

[20] Seifarth, H. et al., 1998. Preparation of SiO2 films with embedded Si nanocrystals by reactive r.f. magnetron sputtering. *Thin Solid Films*, vol. 330(2), pp. 202-205.

[21] G. Yue, et al., "Photoluminescence and Raman studies in thin-film materials: Transition from amorphous to microcrystalline silicon," *Applied Physics Letters*, 1999, vol. 75, pp. 492-494.

[22] Z. Iqbal, S. Veprek, "Raman Scattering From Hydrogenated Microcrystalline and Amorphous Silicon," *J. Phys. C:Solid State Phys.*, 1982, vol. 15, pp. 377-392.